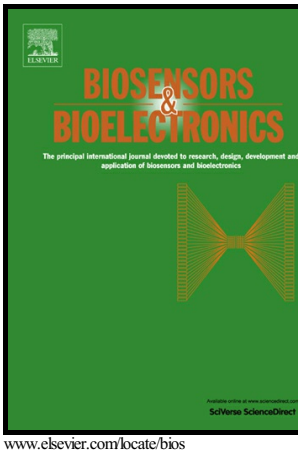

A novel label-free and enzyme-free electrochemical aptasensor based on DNA in situ metallization

Fenglei Gao, Yong Qian, Lili Du, Yu Zhang, Daoquan Tang, Dongzhi Yang

www.elsevier.com/locate/bios

PII: S0956-5663(15)30244-X
DOI: http://dx.doi.org/10.1016/j.bios.2015.06.078
Reference: BIOS7815

To appear in: *Biosensors and Bioelectronic*

Received date: 28 May 2015
Revised date: 27 June 2015
Accepted date: 29 June 2015

Cite this article as: Fenglei Gao, Yong Qian, Lili Du, Yu Zhang, Daoquan Tang and Dongzhi Yang, A novel label-free and enzyme-free electrochemical aptasensor based on DNA in situ metallization, *Biosensors and Bioelectronic* http://dx.doi.org/10.1016/j.bios.2015.06.078

A novel label-free and enzyme-free electrochemical aptasensor based on DNA in situ metallization

Fenglei Gao*, Yong Qian, Lili Du, Yu Zhang, Daoquan Tang, and Dongzhi Yang
Jiangsu Key Laboratory of New Drug Research and Clinical Pharmacy, School of Pharmacy, Xuzhou Medical College, 221004, Xuzhou, China.

Abstract: In this work, we presented a novel label-free and enzyme-free electrochemical aptasensor based on DNA in situ silver metallization as effective electrochemical label. Molecular beacon 2 (MB2, Peptide nucleic acid) was first immobilized on the gold electrode (AuE) through Au-S bond. In the presence of thrombin, the thrombin binding aptamer (MB1) preferred to form thrombin/aptamer complex in lieu of aptamer–DNA duplex, resulting in the 8−17 DNAzyme liberating from the caged structure and hybridization with the MB2, the MB2 will replace and free the target thrombin when it hybridizes with MB1. The released target thrombin can participate in the next hybridization process with MB1. Eventually, each target thrombin went through many cycles, resulting in numerous MB1 confining close to the AuE, which leaded to the surface became negatively charged and allowed the absorption of silver ions on the DNA skeleton. After chemical reduction by hydroquinone, the formed silver nanoparticles could be afforded a signal trace for electrochemical stripping analysis of target thrombin. Through introducing a hybridization chain reaction to increase the DNA length, the current signal was further amplified, achieved the detection of thrombin with a linear range from 1.0×10^{-16} to 1.0×10^{-11} M and a detection limit of 37 aM. In addition, the signal amplification is realized without using any enzymes or sophisticated label process, and the sensing strategy is completely non-labeled. The success in the present biosensor served as a significant step towards the development of monitoring ultratrace thrombin in clinical detection.

Keywords: in situ; metallization; label-free; aptasensor;

*Corresponding author. Tel/Fax: +86-516-83262138.

Email: jsxzgfl@sina.com.

Introduction

Aptamers are artificial, short, single-stranded DNA/RNA oligonucleotides that are selected in vitro by systematic evolution of ligands by exponential enrichment (Xue et al. 2012; Li et al. 2015; Jin et al. 2015; Zheng et al. 2015). Aptamers can successively compete with antibodies as biorecognition elements for biosensors due to their specific properties (Li et al. 2011b; Li et al. 2012; Chen et al. 2014; Lin et al. 2014; Sun et al. 2014; Wang et al. 2015). They can be selected to bind a wide range of targets, including small molecules, proteins or even whole cells with high specificity and affinity (Liu et al. 2014; Bi et al. 2014; Feng et al. 2014; Zhao et al. 2014). They are thermally stable, reusable and can be easily modified for their detection and immobilisation by introducing of functional groups (Wu et al. 2013; Zhang et al. 2013; Li et al. 2014). Compared with anti-bodies (conventional affinity reagents for the target antigen proteins) (Shuman et al. 1976; Bichler et al. 1991; Zhu et al. 2000), aptamers hold many advantageous characteristics, including simple and reproducible synthesis, easy and controllable labeling, long-term stability and design flexibility. Due to these unique features, aptamers have been increasingly used as promising recognition elements alternative to antibodies in designing different including electrochemical (Xiao et al. 2005; Li et al. 2008; He et al. 2007; Zhao et al. 2011; Sun et al. 2014; Baker et al. 2006), fluorescence (Lin et al. 2006; Wang et al. 2004; Huang et al. 2010; Chang et al. 2010; Chi et al. 2011), colorimetry (Huang et al. 2005; Wang et al. 2008; Li et al. 2012; Li et al. 2014), surface plasmon resonance (Wang et al. 2008; Wang et al. 2010), electrochemiluminescence (Huang et al. 2009; Wang et al. 2011; Li et al. 2012)

and surface enhanced Raman spectroscopy (Hu et al. 2008; Li et al. 2012; He et al. 2013) biosensors for the detection of cancer cells, organic molecules, and a variety of proteins. Among these aptasensors, electrochemical aptasensors are the most attractive due to their advantages of fast response, portability, high sensitivity, simple instrumentation, low cost. The coupling of enzymes, redox probe and metal nanoparticles as amplifying labels is a general paradigm advantageous for amplifying electrochemical signals of aptasensors. However, this approach commonly involved in the fussy labeling process and might result in the deactivation of aptamer. Therefore, the enzyme-free and label-free electrochemical aptasensing systems have received increasing interest, due to the simplicity of these sensing approaches without the involvement of any enzymes or modifications to the aptamers to generate the electrochemical signal output. In this paper, we report a novel label-free and enzyme-free electrochemical aptasensor based on DNA in situ metallization.

DNA metallization has evoked substantial research activity in the generation of conductive nanowires and the construction of functional circuits (Braun et al. 1998; Yan et al. 2003). Since DNA has a high affinity for metal cations, this technology provides a route to selectively form metal nanoparticles along with the DNA template (Keren et al. 2004). Moreover, these nanoparticles can be used as nucleation sites for further deposition of metal nanoparticles, such as silver, gold, palladium and platinum nanoparticles (Ford et al. 2001; Liu et al. 2004; Ongaro et al. 2005; Liu et al. 2006). These DNA-based nanomaterials hold promise for application in nanodevices and biosensors. In this work, the electrochemical stripping of DNA meditated Ag

nanoparticles was used to produce an electrochemical signal.

In order to further improve the sensitivity of electrochemical detection in these aptasensors, many signal amplification strategies are employed, such as polymerase chain reaction (Zhang et al. 2012), strand displacement amplification (Cheng et al. 2012), rolling circle amplification (Cheng et al. 2012), loop-mediated isothermal amplification(Liang et al. 2012), the isothermal exponential amplification (Zhang et al. 2012) and nicking endonuclease or exonucleases (Liu et al. 2011) assisted signal amplification and so on. Among these methods, the hybridization chain reaction (HCR) (Zhu et al. 2015) and target-catalyzed hairpin assembly (Huang et al. 2012; Qian et al. 2015) attracted researchers' considerable attention to design sensitive assays for the analysis of targets. During these amplification approaches, self-assembly of DNA hairpins can be triggered by single-stranded DNA through strand displacement reaction, which is driven by the free energy of base pair formation without enzyme. Till now, it has widely been employed for the analysis of nucleic acid, protein and small molecules by coupling with electrochemistry, electroluminescence, fluorescence, and colorimetry.

Herein, a simple, isothermal, enzyme-free and label-free ultrasensitive electrochemical aptasensor platform was proposed based on the ingenious combination of target catalyzed hairpin assembly and HCR strategies for two-step signal amplification. To demonstrate the utility of our approach, human thrombin is chosen as the target, which plays an important role in the coagulation cascade, thrombosis and hemostasis. The DNA hairpin assembly on the electrode is triggered by target thrombin accompanying the release of target thrombin for the successive assembly process. Then,

the initiator capture probe and two hairpin helper DNAs lead to the formation of extended dsDNA polymers through HCR on the electrode surface. The electrochemical signal was originated from the electrostatic collection of silver cations along the DNA duplex, the reductive formation of silver nanoparticles along the DNA backbone, and stripping potentiometric detection of the silver nanoparticles. Notably, the label-free strategy eliminates the requirement for labeling, making the system more simple and cost effective. The proposed strategy provides a simple, high selective versatile platform for target detection.

2. Materials and methods

2.1. Materials and reagents

Sulfuric acid (70%), toluene, ammonium hydroxide (25%), $AgNO_3$, and 6-mercaptohexanol (MCH) were obtained from Shanghai Reagent Co. (Shanghai, China). Thrombin, tris (2-carboxyethyl) phosphane hydro-chloride (TCEP), immunoglobulin G (IgG), hemoglobin (Hb), and lysozyme and hydroquinone were obtained from Sigma−Aldrich Inc. Phosphate buffer saline (PBS) was prepared by mixing the stock solutions of NaH_2PO_4 and Na_2HPO_4 (10 mM, pH 7.4). DNA hybridization buffer was phosphate-buffered saline (137 mM NaCl, 2.5 mM Mg^{2+}, 10 mM Na_2HPO_4, and 2.0 mM KH_2PO_4, pH 7.4). The citrate buffer was prepared by mixing the stock solutions of citric acid and sodium citrate (0.1 M, pH 3.5). Human serum samples were kindly provided by Jiangsu Cancer Hospital (Nanjing, China). A mixture containing equal volumes of human serum sample and DNA hybridization buffer was used for recovery testing. Ultrapure water obtained from a Millipore water

purification system (18 MΩ, Milli-Q, Millipore) was used in all assays. PNA was purchased from Chengdu CP Biochem Co., Ltd. (Chengdu, China). DNA oligonucleotides were synthesized and purified by Takara Biotechnology Co., Ltd. (Dalian, China) and stored in DNA hybridization buffer. The sequences of these oligonucleotides are as follows:

MB1: 5'-AGTCCGTGGTAGGGCAGGTTGGGGTGACTTTTTACCACGGACT GTTATTAATGTGTGATGT -3'

MB2 (Peptide nucleic acid): 5'-AGTCCGTGGTAAAAAGTCACCCCAACCTGCCC TACCACGGGGTGACTTTTTACCA-SH-3'

H1: 5'-ACATCACACATTAATAACCTACCATCGCACTTAGAT-3'

H2: 5'-GTTATTAATGTGTGATGTATCTAAGTGCGATGGTAG-3'

Fluorophore-linker-MB1:

5'-FAM-AGTCCGTGGTAGGGCAGGTTGGGGTGACTTTTTACCACGGACT GTTATTAATGTGTGATGT-3'—BHQ

2.2 DNA Self-assembly on gold electrode and silver deposition.

Prior to modification, the bare AuE (3 mm in diameter) was polished to a mirror-like surface with alumina suspensions and then sequentially cleaned ultrasonically in 95% ethanol and twice-quartz-distilled water for 5 min. Prior to attachment to the AuE surface, 100 μL of 100 μM thiolated MB2 was incubated with 0.1 μL of 100 mM TCEP for 1 h to reduce disulfide bonds and subsequently diluted to 1.0 μM with phosphate buffer. 10 μL of thiolated MB2 (1 μM) was dropped on the cleaned AuE for 2 h at room temperature in the dark. During this process, the MB2 was

conjugated onto the AuE via the Au–S bond. After rinsing with distilled water, the modified AuE was incubated with 1.0 mM MCH in10 mM Tris–HCl buffer (pH7.4) for 1 h at room temperature. MB1 (300 nM, 25 μL) mixed with different concentrations of human thrombin were dropped on the surface of the electrode. After the process was performed for 2 h at 37 °C, it was terminated by washing thoroughly. To amplify the electrochemical signal, a mixture of 10 μL of H1 (10 μM) and 10 μL of H2 (10 μM) was dropped on the surface of the electrode and incubated for 100 min to complete the long-range self-assembly. When the assembly finished, the resulting electrode was again thoroughly rinsed and dried before electrochemical characterization.

The DNA-template induced generation of silver nanoparticles was based on an earlier procedure. The electrostatic collection of silver ion was preceded by soaking the resulting DNA-modified electrode in an ammonium hydroxide (pH 10.5) solution containing 0.1 M $AgNO_3$. Metallization of the collected silver was carried out (after a vigorous washing) by dipping the electrode in an ammonium hydroxide (pH 10.5) medium containing 0.05 M hydroquinone (in the absence of silver in the solution). Each of the above processes was carried out for 10 min in the dark. After silver deposition, the electrode was rinsed with water and LSV from -0.15 to 0.25 V at 50 mVs^{-1} was performed in a 1 .0 M KCl solution.

2.3 Application of the thrombin aptasensor in the biological assay

Human whole blood was provided by the local hospital. After the natural coagulation, the blood was centrifugated and the supernatant was obtained to be used. The actual samples were prepared by mixing different concentrations of thrombin. All

the experiment conditions were the same as the target detection.

2.4 Measurement procedure

Linear sweep stripping voltammetric (LSV) measurements were performed using a CHI 660B electrochemical workstation (CHI, Shanghai, China) at room temperature using a conventional three-electrode system with a modified AuE as the working electrode, a platinum wire as the auxiliary, and a saturated calomel electrode as the reference. Electrochemical impedance spectroscopic (EIS) analysis was performed with an Autolab PGSTAT12 (Ecochemie) in 0.1M KCl containing 5 mM $K_4[Fe(CN)_6]/K_3[Fe(CN)_6]$. Tapping mode atomic force microscopic (AFM) image was acquired under ambient conditions using an Agilent 5500 AFM/SPM system. X-ray photoelectron spectroscopic (XPS) measurements were performed using an ESCALAB 250 spectrometer (Thermo-VG Scientific) with an ultrahigh vacuum generator.

3. Results and discussion

3.1. The principle of enzyme-free and label free aptasensor for amplification detection of human thrombin.

Scheme 1 depicts the principles of the analytical process for amplification detection of human thrombin. This work first immobilized MB2 (Peptide nucleic acid) on the AuE through Au-S bond. In the presence of thrombin, the thrombin binding aptamer (MB1) preferred to form thrombin/aptamer complex in lieu of aptamer–DNA duplex, resulting in the disassembly of the original duplex MB1. Owing to the MB1-MB2 duplex is more stable than the target thrombin–MB1 hybrids; the MB2 will replace and free the target thrombin when it hybridizes with MB1. The released target

thrombin can participate in the next hybridization process with MB1. Hence, each copy of target can trigger numerous assembly processes between MB1 and MB2, and can be indicated as target catalyzed hairpin assembly strategy. In the absence of target, the MB1 and MB2 can only maintain the sufficiently stable stem-loop structure owing to the binding of the complementary sequences at the ends. After target catalyzed hairpin assembly between MB1 and MB2 on the electrode surface, the newly emerging DNA fragment (the sticky end of MB2) on the electrode is further used to propagate the HCR between H1 probe and H2 probe, inducing are markably amplified electrochemical signal. Due to the negative phosphate backbone of the DNA, the positively charged silver ions were introduced onto the AuE through electrostatic interactions. Followed by hydroquinone reduction, Ag nanoparticles are formed along with the DNA skeleton. Then, the Ag NPs analyzed by LSV could avoid the requirement of deoxygenation, which makes the electrochemical detection of thrombin simple and sensitivity.

3.2. Verification of biosensor fabrication process.

To estimate the signal amplification function of the proposed biosensor, we have investigated and compared the electrochemical performances of the sensor under different conditions. As shown in Fig. 1A, no reduction peak could be observed for the MB2 immobilized electrode (curve a) in the absence of target thrombin, indicating no silver nanoparticle was deposited on the substrate surface due to the backbone of peptide nucleic acid MB2 was neutral. In contrast, after target DNA was added and following silver deposition, the resulting electrode showed an obvious stripping peak

(curve b), it is because that the MB2 was designed to displace the target protein through a process similar to DNA branch migration (Li et al. 2011a). Subsequently, the current intensity increased with the reaction time (curve c). Clearly, the signal enhancement was caused by the cycling use of the target thrombin and the continuous generation of the MB1−MB2 complex as shown in Scheme 1, which allowing much of the MB1 to approach the electrode surface for deposition more Ag NPs. Subsequently, the electrode is further used to propagate the HCR between H1 probe and H2 probe, it appears an obvious stripping peak (curve d), which was 2.75 times greater than that in the absence of HCR. Because the HCR could increase the length of the DNA for deposition more silver nanoparticles, resulting in amplifying electrochemical signal output. Thus, the proposed aptasensor can be used for the amplified detection of protein, which supports the concept for the analysis process suggested in Scheme 1.

To verify that the binding force of double stranded DNA hybridization would release target protein thrombin from target-aptamer complex, hybridization tests using free DNA strands in solution were performed. A fluorophore and a quencher were added on the MB1. As shown in Fig. 1B, by itself or in the absence of target thrombin, a weak fluorescence emission was observed (curve a) since the fluorescence of FAM was quenched by the black hole quencher (BHQ). However, upon addition of target thrombin, an enhanced fluorescence peak was observed (curve b), indicating that binding of thrombin to the aptamer induced conformational change of the aptamer, increasing the distance between the fluorophore and the quencher and therefore reducing the quenching effect and producing fluorescence. The fluorescence of MB1

was obviously increased upon the addition of target thrombin and MB2 (Fig. 1B, curve c). Upon the addition of target protein, the opening of the hairpin structure of MB1 is facilitated, making the region II available for hybridization with the region III of MB2. Then, the target protein can be displaced from hairpin MB1 by hairpin MB2 through a process similar to DNA branch migration, the released target can then interact with another MB1, and the cycle starts anew. In this way, a single target can generate many MB1-MB2 complexes, which leads to the significant fluorescence enhancement, indicating that the binding force between MB1 and MB2 must be strong enough and would release target protein thrombin from target-aptamer complex. In addition, for the solution containing MB2 only, the fluorescence intensity was not changed (curve d) compare to the blank (curve a), indicating that the hairpin structures of MB2 could not open the loop of MB1 owing to the binding of the complementary sequences at the ends.

3.2. Characterization of the biosensor.

EIS has been applied to characterize the electrodes at different stages. The equivalent circuit as the model of the work electrode (shown in the top right corner of Fig. 1C) was used to offer a direct way for us to get more information from EIS results. This contains the electrolyte solution resistance Rs, the surface electron transfer resistance Rct that reflects the surface property of surface of the electrode, the Warburg impedance Zw and the constant phase element related to double layer capacitance Cdl. As shown in Fig. 1C, the bare Au electrode shows nearly no semicircle domain (curve a), indicating that the electroactive ion of $[Fe(CN)_6]^{3-/4-}$ is transported fast on the

electrode interface. After thiolated capture MB2 self-assembled onto the electrode surface, the Rct increased significantly (curve b), because the oligonucleotides were non-electroactive, the resistance of electron-transfer was strong. The value of Rct further increases by the blocking of the electrode with MCH (curve c). It is noted that the interaction of thrombin with its aptamer H1 dropped to the AuE surface causes a large increase in the Rct (curve d) due to the steric effect of thrombin and the conformational change of H2. The Rct largely increased with the time due to the cycling use of the target thrombin and the continuous generation many of the MB1−MB2 complexes (curve e). Subsequently, a large semicircle domain was observed when the electrode was incubated with the H1 and H2 for HCR (curve f), indicating a high resistance of the electrode interface as the double helices copolymers that obstruct the electron transfer of the electrochemical probe. However, the Rct decreased when the Ag NPs were attached to the DNA due to the excellent electronic conductivity of Ag NPs (curve g). The impedance experiments demonstrated that the DNA sensor had been successfully created by the HCR.

The morphology of the prepared Ag-NPs was investigated by AFM, which provided the direct evidence of the formation of Ag NPs. As shown in Fig. 2A, the Ag nanoparticles growth was observed only along the DNA, and no background Ag deposition was presented, because only the free anionic phosphate group of DNA backbone was expected to form the DNA−Ag^+ complex through electrostatic interaction. In addition, XPS was employed to confirm that the element of the NPs within the DNA helix is Ag single matter. P (2p) peak occurred at 133.1 eV, which

corresponded to the phosphate group, confirming the assembly of DNA on GE. Compared with electrode without silver deposition, the XPS of DNA-PNA modified electrode showed two new strong peaks at 374 and 368 eV (Fig. 2B) after Ag deposition, which correspond to Ag (3d), respectively, confirming the deposition Ag NPs on the electrode surface. These results indicated that the formation and growth of Ag nanoparticles on the DNA backbone could as electro-tags for subsequent electrochemical detection.

3.3. Optimization of the reaction conditions.

The reaction conditions play an important role in the sensing process, such as the MB2 concentration and the incubation time. In order to achieve the best signal-to-noise level, the reaction conditions were optimized. To investigate the effect of the concentration of MB1 on the detection system, target thrombin (10 fM) was mixed with MB1 at different concentrations ranging from 0 to 400 nM. As shown in Fig. 3A, the current intensity of the system increased as the concentration of MB1 increased. Furthermore, the optimum concentration of MB1 used in this system was 300 nM due to its best signal-to-noise level. As shown in Fig. 3B, it could be found that the electrochemical signal increased with the reaction time before reaching saturation after 2 h, indicating strongly that target thrombin could go through many cycles to open the MB1. Considering this issue, 2 h was chosen as the reaction time. The maximum peak current was observed when the HCR reaction was maintained at about 100 min (Fig. 3C). As shown in Fig. 3D, the intensity increased with the increasing silver deposition time due to the increasing amount of silver nanoparticles deposition on the DNA

skeleton. The intensity reached a maximum value at 10 min.

3.4. Analytical performance of the aptasensor.

Under the optimal detection condition, the dynamic linear range of the fabricated aptasensor toward thrombin standards was evaluated by LSV experiment in 2 mL KCl (1 M). As shown in Fig. 4A, the electrochemical signal increased with increasing concentrations of thrombin as a result of the efficient deposit of Ag NPs. Accordingly, Fig. 4B displayed that the reduction peak current was linearly dependent on the logarithm of thrombin concentration in the range of 1 fM–10 pM. The regression equation is I = 12.86 log C + 197.42 with a correlation coefficient of 0.9982, where I and C represent the intensity and the thrombin concentration, respectively. Also, a detection limit of 0.54 fM (a signal-to-noise ratio of 3) was obtained. To achieve higher detection sensitivity, HCR amplification was introduced to the detection protocol (Scheme 1, b). HCR is an enzyme-free process where the hybridization event is triggered by target DNA as an initiator to produce oligonucleotide polymerization. It can achieve about 10-fold amplification at a constant temperature within a reaction time of 2 h. After HCR, longer double-stranded DNA was generated for absorbing more Ag^{+} cation and producing more silver nanoparticles, which led to a substantial increase in the corresponding electrochemical intensity. At the same target thrombin concentrations of 1 fM and 1 pM, the electrochemical intensity with HCR (Fig. 5A) was 4.4 and 2.22 times higher than those without HCR amplification (Fig. 4A), respectively. The HCR process produced a linear range from 1.0×10^{-16} to 1.0×10^{-11} M for electrochemical detection of target thrombin (Fig. 5B) (The regression equation

is I = 24.24 log C + 386.62 with a correlation coefficient of 0.9943). The limit of detection at 3σ was 37 aM, which was 14.6-fold lower than that without HCR amplification. Additionally, detection performances of the proposed method were compared with that of other approaches for thrombin detection and the results were shown in Table 1. Such comparison reflected that the proposed aptasensor exhibited much higher sensitivity, which provided a powerful evidence of our strategy for ultrasensitive detection of thrombin. The above results indicated the successful achievement of the electrochemical amplified thrombin detection, which should be attributed to three factors: (1) target-catalyzed hairpin assembly assisted thrombin recycling for formation of many MB1 stems to trigger HCR, (2) highly loaded Ag NPs on the surface of electrode by HCR, and (3) the stripping analysis of deposited silver. Thus the results identified that this signal amplification method was efficient for ultrasensitive electrochemical detection of thrombin.

3.5. Specificity and reproducibility of the aptasensor.

To evaluate the selectivity of the aptasensor, three other non-target proteins were tested and the results were exhibited in Fig. 6. The presence of even 100-fold excess of non-target proteins, mouse IgG (1 pM), Hb (1 pM), and lysozyme (1 pM), and causes insignificant current increase compared with that of the blank test. However, the presence of 10 fM thrombin results in a significant increase in the current response. The results showed that the presence of mouse IgG, Hb, and Lyso did not induce any great changes of signal. Similarly, a mixed sample (10 fM thrombin coexisted with high concentration of interfering components mouse IgG (0.1 nM), Hb (0.1 nM), and

Lysozyme (0.1 nM) did not display large signal change compared with that of thrombin alone. This comparison essentially suggested that the aptasensor was highly selective and had quite an affinity toward thrombin.

The reproducibility of the aptasensor was examined through the following methods: four of the same batch aptasensors were used to detect 10 fM thrombin under the same experimental condition, all of the four aptasensors showed analogous electrochemical signals achieving a relative standard deviation (RSD) of 3.4%. Similarly, the same aptasensor was used to detect 10 fM thrombin for four times. A RSD of 4.4% could be got, demonstrating that the reproducibility of the aptasensor was acceptable.

3.6. Analytical application of the aptasensor.

To assess the analytical reliability and application of the proposed aptasensor, recovery experiments are performed by standard addition methods in human serum. A series of samples are prepared by adding thrombin of different concentrations into healthy human serum samples. Then, the obtained samples are analyzed by the proposed aptasensor and the results are given in Table 2. The range of variation of the recovery is from 95.7 % to 106.8% and the relative standard deviation is between 4.3% and 6.4%. These results indicate that the proposed electrochemical aptasensor provided a potential application in real biological samples.

4. Conclusions

In summary, we have demonstrated the construction of a label free and enzyme free electrochemical aptasensor for detection of thrombin based on target catalyzed

hairpin assembly, HCR and DNA in situ metallization. On the basis of dual signal amplification strategy, the prepared aptasensors exhibited high response sensitivity with a linear range from 1.0×10^{-16} to 1.0×10^{-11} M and a detection limit of 37 aM. The current strategy avoids the use of any kind of enzyme and sophisticated label process. The electrochemical oxidation of Ag NPs in KCl excluded specific detection conditions, such as pretreatment of the NPs, high stripping potential, and deoxygenation procedure. Therefore, the method presented here provided a universal platform to detect protein at an ultrasensitive level in biomedical and bioanalytical applications.

Acknowledgment

This work was supported by the National Natural Science Foundation of China (21405130), Excellent Talents of Xuzhou Medical College (D2014007), State Key Laboratory of Analytical Chemical for Life Science (SKLACLS1405) and Most Foundation of Jiangxi Province (20152ACB21018).

References

Bichler, J., Siebeck, M., Maschler, R., Pelzer, H., Fritz, H., 1991. Blood Coagul. Fibrinolysis 2, 129–133.

Braun, E., Eichen, Y., Sivan, U., Ben-Yoseph, G., 1998. Nature 391, 775−778.

Baker, B.R., Lai, R.Y., Wood, M.S., Doctor, E.H., Heeger, A. J., Plaxco, K.W., 2006. J. Am. Chem. Soc. 128, 3138–3139.

Chen, Z.B., Tan, Y., Zhang, C.M., Yin, L., Ma, H., Ye, N.S., Qiang, H., Lin, Y.Q., 2014. Biosens. Bioelectron. 56, 46–50.

Cheng, W., Zhang, W., Yan, Y.R., Shen, B., Zhu, D., Lei, P.H., Ding, S.J., 2014. Biosens. Bioelectron. 62, 274–279.

Chang, H.X., Tang, L.H., Wang, Y., Jiang, J.H., Li, J.H., 2010. Anal. Chem. 82, 2341–2346.

Chi, C.W., Lao, Y. H., Li, Y.S., Chen, L.C., 2011. Biosens. Bioelectron. 26, 3346–3352.

Feng, L.Y., Zhang, Z.J., Ren, J.S., Qu, X.G., 2014. Biosens. Bioelectron. 62, 52–58.

Ford, W.E., Harnack, O., Yasuda, A., Wessels, J.M., 2001. Adv. Mater. 13, 1793−1797.

He, P., Shen, L., Cao, Y., Li, D., 2007. Anal. Chem. 79, 8024–8029.

He, P., Zhang, Y., Liu, L.J., Qiao, W.P., Zhang, S.S., 2013. Chem. Eur. J. 19, 7452−7460.

Hu, J., Zheng, P.C., Jiang, J.H., Shen, G.L., Yu, R.Q., Liu, G.K., 2008. Anal. Chem. 81, 87–93.

Huang, D.W., Niu, C.G., Qin, P.Z., Ruan, M., Zeng, G.M., 2010. Talanta 83, 185–189.

Huang, C.C., Huang, Y.F., Cao, Z., Tan, W., Chang, H.T., 2005. Anal. Chem. 77, 5735–5741.

Huang, H.P., Zhu, J.J., 2009. Biosens. Bioelectron. 25, 927–930.

Huang, J.H., Su, X.F., Li, Z.G., 2012. Anal. Chem. 84, 5939–5943.

Jin, G.X., Wang, C.M., Yang, L.L., Li, X.J., Guo, L.H., Qiu, B., Lin, Z.Y., Chen, G.N., 2015. Biosens. Bioelectron. 63, 166–171.

Keren, K., Berman, RS., Braun, E., 2004. Nano Lett. 4, 323−326.

Li, B.L., Wang, Y.L., Wei, H., Dong, S.J., 2008. Biosens. Bioelectron. 23, 965–970.

Li, B., Ellington, A.D., Chen, X., 2011a. Nucleic Acids Research 39, e110.

Li, Y.F., Bao, J.C., Han, M., Dai, Z.H., Wang, H.S., 2011b. Biosens. Bioelectron. 26, 3531–3535.

Li, Y.F., Liu, L.L., Fang, X.L., Bao, J.C., Han, M., Dai, Z.H., 2012. Electrochim. Acta 65, 1–6.

Li, J., Li, W., Qiang, W.B., Wang, X., Li, H., Xu, D.K., 2014. Anal. Chim. Acta 807, 120–125.

Li, Y.F., Liu, L.L., Fang, X.L., Bao, J.C., Han, M., Dai, Z.H., 2012. Electrochim. Acta 65, 1–6.

Li, J., Fu, H.E., Wu, L.J., Zheng, A.X., Chen, G.N., Yang, H.H., 2012. Anal. Chem. 84, 5309–5315.

Li, Y., Lei, C.C., Zeng, Y., Ji, X.T., Zhang, S.S., 2012. Chem. Commun. 48, 10892–10894.

Li, S.Y., Chen, D.Y., Zhou, Q.H., Wang, W., Gao, L.F., Jiang, J., Liang, H.J., Liu, Y.Z., Liang, G.L., Cui, H., 2014. Anal. Chem. 86, 5559–5566.

Li, S.G., Zhu, W., Xue, Y.C., Liu, S.Q., 2015. Biosens. Bioelectron. 64, 611–617.

Lin, X.X., Chen, Q.S., Liu, W., Li, H.F., Lin, J.M., 2014. Biosens. Bioelectron. 56, 71–76.

Liu, S.F., Lin, Y., Liu, T., Cheng, C.B., Wei, W.J., Wang, L., Li, F., 2014. Biosens. Bioelectron. 56, 12–18.

Lin, C., Katilius, E., Liu, Y., Zhang, J., Yan, H., 2006. Angew. Chem. Int. Ed. 45, 5296–5301.

Liu, D., Park, S.H., Reif, J.H., LaBean, T.H., 2004. Proc. Natl. Acad. Sci. U.S.A. 101, 717−722.

Liu, H.P., Chen, Y., He, Y., Ribbe, A.E., Mao, C.D., 2006. Angew. Chem., Int. Ed. 45, 1942−1945.

Liu, Z.Y., Zhang, W., Zhu, S.Y., Zhang, L., Hu, L.Z., Parveen, S., Xu, G.B., 2011. Biosens. Bioelectron. 29, 215–218.

Liang, C., Chu, Y.N., Cheng, S.J., Wu, H.P., Kajiyama, T., Kambara, H., Zhou, G.H., 2012. Anal. Chem. 84, 3758–3763.

Ongaro, A., Griffin, F., Beeeher, P., Nagle, L., Iacopino, D., Quinn, A., Redmond, G., Fitzmaurice, D., 2005. Chem. Mater. 17, 1959−1964.

Qian, Y., Tang, D.Q., Du, L.L., Zhang, Y.Z., Zhang, L.X., Gao, F.L., 2015. Biosens. Bioelectron. 64, 177-181.

Shuman, M.A., Majerus, P.W., 1976. J. Clin. Invest. 58, 1249–1258.

Sun, A.L., Qi, Q.G., Wang, X.N., Bie, P., 2014. Biosens. Bioelectron. 57, 16–21.

Wu, L., Zhang, X.H., Liu, W., Xiong, E.H., Chen, J.H., 2013. Anal. Chem. 85, 8397–8402.

Wang, X.L., Li, F., Su, Y.H., Sun, X., Li, X.B., Schluesener, H.J., Tang, F., Xu, S.Q., 2004. Anal. Chem. 76, 5605–5610.

Wang, J.L., Zhou, H.S., 2008. Anal. Chem. 80, 7174–7178.

Wang, Y.L., Li, D., Ren, W., Liu, Z.J., Dong, S.J., Wang, E.K., 2008. Chem. Commun. 22, 2520–2522.

Wang, J.L., Munir, A., Zhu, Z.Z., Zhou, H.S., 2010. Anal. Chem. 82, 6782–6789.

Wang, J., Shan, Y., Zhao, W.W., Xu, J.J., Chen, H.Y., 2011. Anal. Chem. 83, 4004–4011.

Wang, Y., Yuan, R., Chai, Y.Q., Yuan, Y.L., Bai, L.J., 2012. Biosens. Bioelectron. 38, 50–54.

Wu, Y.M., Xu, W.J., Bai, L.J., Yuan, Y.L. Yi, H.Y., Chai, Y.Q., Yuan, R., 2013. Biosensors and Bioelectronics 50, 50–56.

Wang, K.Y., Liao, J., Yang, X.Y., Zhao, M., Chen, M., Yao, W.R., Tan, W.H., Lan, X.P., 2015. Biosens. Bioelectron. 63, 172–177.

Xiao, Y., Arica, A.L., Alan, J.H., Kevin, W.P., 2005. Angew. Chem. Int. Ed. 44, 5456–5459.

Xue, L. Y., Zhou, X. M., Xing, D., 2012. Anal. Chem. 84, 3507–3513.

Yan, H., Park, S.H., Finkelstein, G., Reif, J.H., LaBean, T.H., 2003. Science 301, 1882−1884.

Yi, H.Y., Xu, W.J., Yuan, Y.L., Wu, Y.M., Chai, Y.Q., Yuan, R., 2013. Biosens. Bioelectron. 47, 368–372.

Zhu, H., Klemic, J.F., Chang, S., Bertone, P., Casamayor, A., Klemic, K.G., Smith, D., Gerstein, M., Reed, M.A., Snyder, M., 2000. Nat. Genet. 26, 283–289.

Zhao, J., Chen, G.F., Zhu, L., Li, G.X., 2011. Electrochem. Commun. 13, 31–33.

Zhao, J., Hu, S.S., Zhong, W.D., Wu, J.G., Shen, Z.M., Chen, Z., Li, G.X., 2014. ACS Appl. Mater. Interfaces 6, 7070–7075.

Zhang, Y., Zhang, C.Y., 2012. Anal. Chem. 84, 224–231.

Zhang, W.Y., Zhang, W.H., Liu, Z.Y., Li, C., Zhu, Z., Yang, C.Y., 2012. Anal. Chem. 84, 350–355.

Zhang, D.W., Nie, J., Zhang, F.T., Xu, L., Zhou, Y.L., Zhang, X.X., 2013. Anal. Chem. 85, 9378–9382.

Zheng, Y.N., Yuan, Y.L., Chai, Y.Q., Yuan, R., 2015. Biosens. Bioelectron. 66, 585–589.

Zhu, Q., Chai, Y.Q., Zhuo, Y., Yuan, R., 2015. Biosens. Bioelectron. 68, 42–48.

Figure captions

Scheme 1 Schematic illustration of label-free and enzyme-free electrochemical aptasensor based on DNA in situ silver metallization without (a) and with (b) HCR amplification.

Fig. 1 (A) LSV curves of Ag NPs deposited at sensor surface (50 mVs^{-1} in 1.0 M KCl) (a) blank, (b) in the presence of 10 pmol L^{-1} target thrombin + MB1, (c) in the presence of 10 pmol L^{-1} target thrombin + MB for 2h, (d) in the presence of 10 pmol L^{-1} target thrombin + MB1 and HCR. (B) Fluorescence spectra of (a) fluorophore-linker-MB1 (100 nM); (b) fluorophore-linker-MB1 (100 nM) and human thrombin (20 nM); (c) fluorophore-linker-MB1, human thrombin (20 nM) and MB2 (100 nM); and (d) fluorophore-linker-MB1 (100 nM) and MB2 (100 nM). Inset: Schematic representation of fluorescence verification strategy. (C) Electrochemical impedance spectra of the different modified electrodes in 0.1 M KCl aqueous solution containing 5 mM (1:1) $[Fe(CN)_6]^{3-/4-}$. (a) Bare GE, (b) MB2/GE, (c) MCH/MB2/GE, (d) target thrombin + MB1/MCH//MB2/GE, (e) (d) for reacting 2h, (f) (d) after HCR, and (g) (f) after silver deposition.

Fig. 2 (A) AFM height image of DNA−PNA duplex modified GE followed with HCR, silver deposition; (B) XPS spectra of DNA−PNA duplex modified GE followed with HCR without (a) and with (b) silver deposition.

Fig. 3 Dependence of LSV responses current intensity on (A) the amount of MB1 for (a) 10 fM target thrombin, (b) no target; (B) the reaction time of target thrombin-catalyzed hairpin assembly for (a) 10 fM target thrombin, (b) no target; (C) the reaction time of HCR, and (D) the silver deposition time. All parameters have HCR steps before the measurement and when one parameter changes the others are under their optimal conditions.

Fig. 4 (A) LSV responses and (B) calibration curve of the aptasensor in 1 M KCl after incubation with target thrombin ranging from 10^{-16} to 10^{-11} mol L^{-1} (curves (a)–(f)) without HCR amplification. Scan rate: 50 mV/s.

Fig. 5 (A) LSV curves of Ag NPs for detection of thrombin after HCR amplification at target concentrations of 10^{-17}–10^{-11} mol L^{-1} (curves (a)–(g)); (B) linear relationship between peak current and the logarithm of target thrombin concentration.

Fig. 6 Histograms of the selectivity of the aptasensor examined by being incubated in the following samples under the same experimental conditions: (a) blank; (b) 1.0 pM Hb; (c) 1.0 pM IgG; (d) 1.0 pM lysozyme; and (e) 10 fM thrombin + 0.1 nM Hb; (f) 10 fM thrombin + 0.1 nM IgG; (g) 10 fM thrombin + 0.1 nM lysozyme; (h) 10 fM thrombin.

Table 1. Comparing of the proposed method with the thrombin assays using aptamer as a recognition molecule.

Analytical method	Detection limit	Linear range	Refs.
Electrochemical	1.7 pM	5 pM to 100 nM	Yi et al. 2013
Electrochemical	0.05 pM	0.15 pM to 40 nM	Wu et al. 2013
Electrochemical	2.7 fM	8 fM to 15 nM	Wang et al. 2012
Electrochemical	37 aM	0.1 fM to 10 pM	This work

Table 2. Determination of thrombin added in human blood serum (n=5) with the proposed aptasensor.

Serum samples	Concentration of thrombin added	Concentration obtained with aptasensor	RSD (%)	Recovery (%)
1	10 pM	9.57 pM	5.6	95.7
2	1 pM	0.97 pM	4.3	97
3	0.1 pM	0.104 pM	5.5	104
4	10 fM	9.84 fM	6.4	98.4
5	1 fM	1.068 fM	5.7	106.8

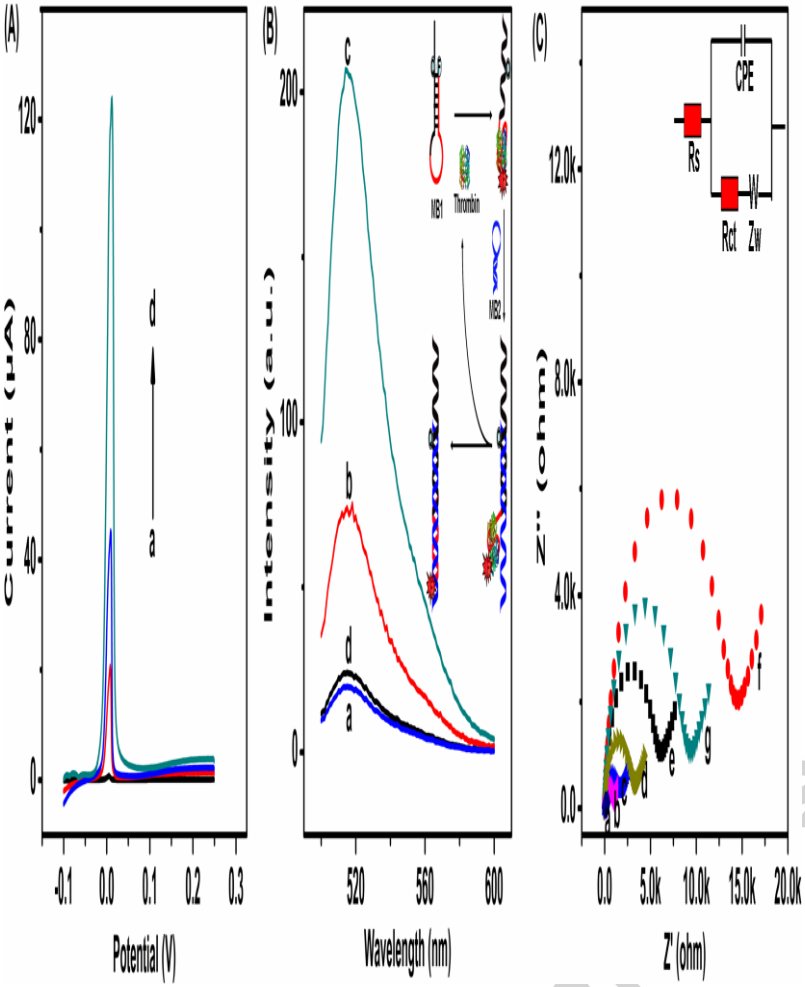

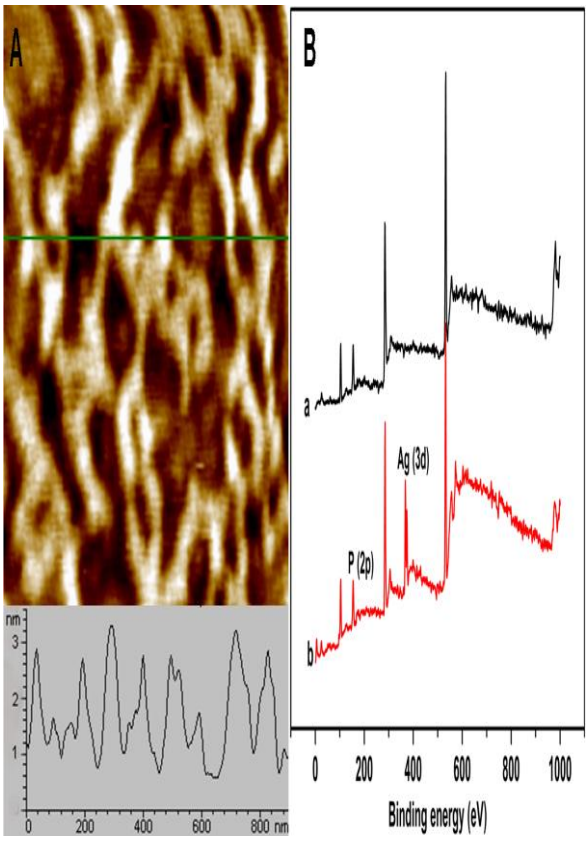

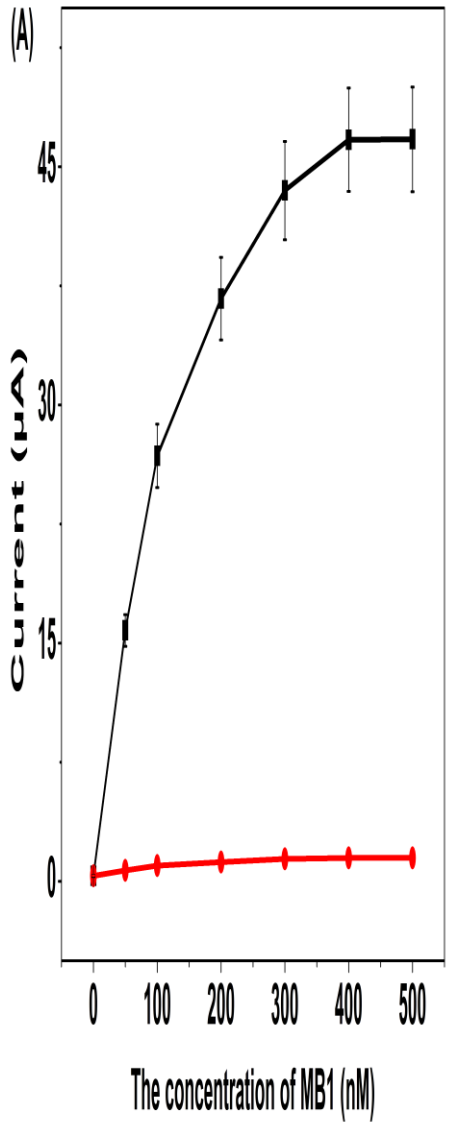
(A)
Current (μA)
0
15
30
45
0
100
200
300
400
500
The concentration of MB1 (nM)

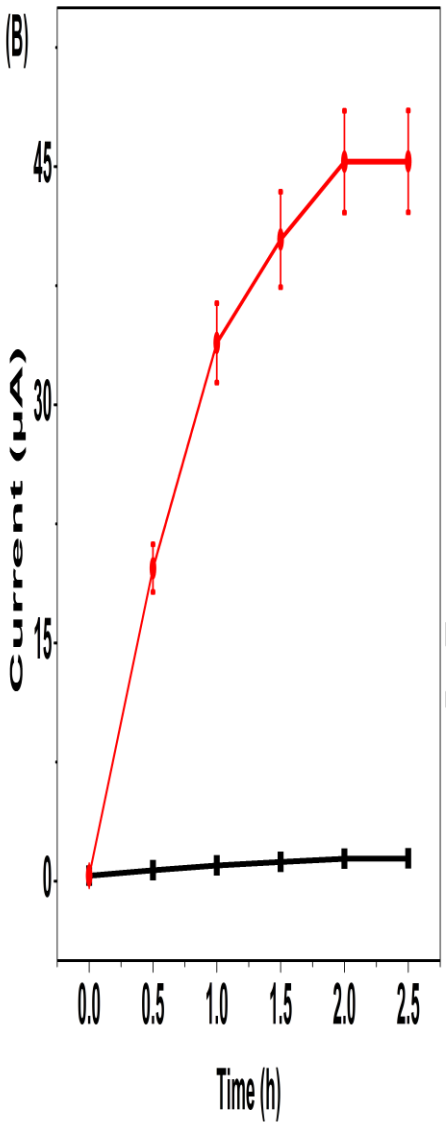
(B)
Current (μA)
0
15
30
45
0.0
0.5
1.0
1.5
2.0
2.5
Time (h)

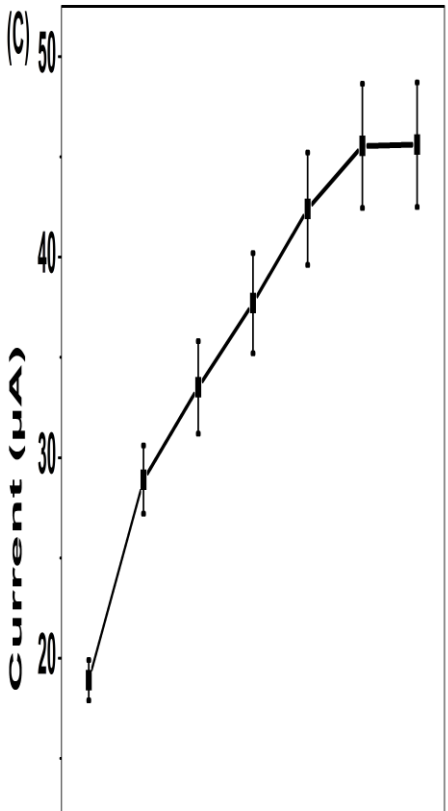
(C)
Current (μA)
20
30
40
50

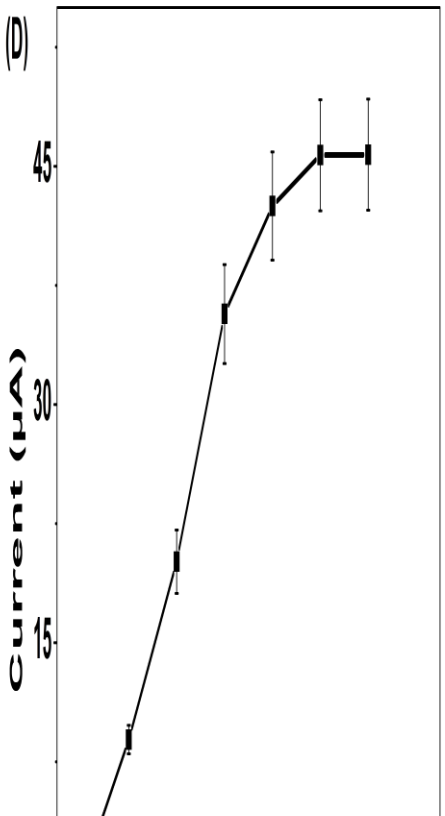
(D)
Current (μA)
15
30
45

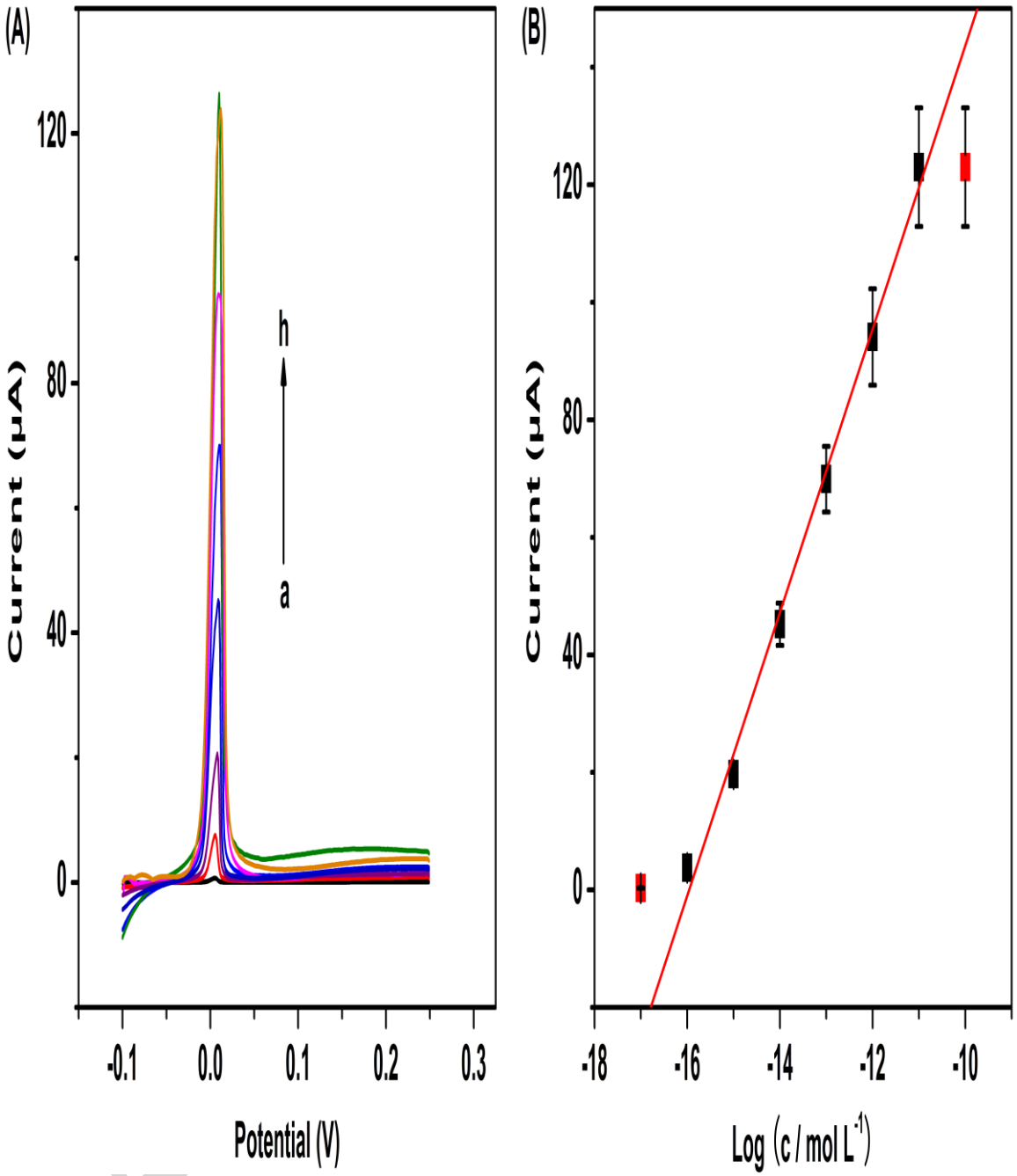
(A)
120
80
40
0
Current (μA)
h
a
-0.1
0.0
0.1
0.2
0.3
Potential (V)
(B)
120
80
40
0
Current (μA)
-18
-16
-14
-12
-10
Log (c / mol L-1)

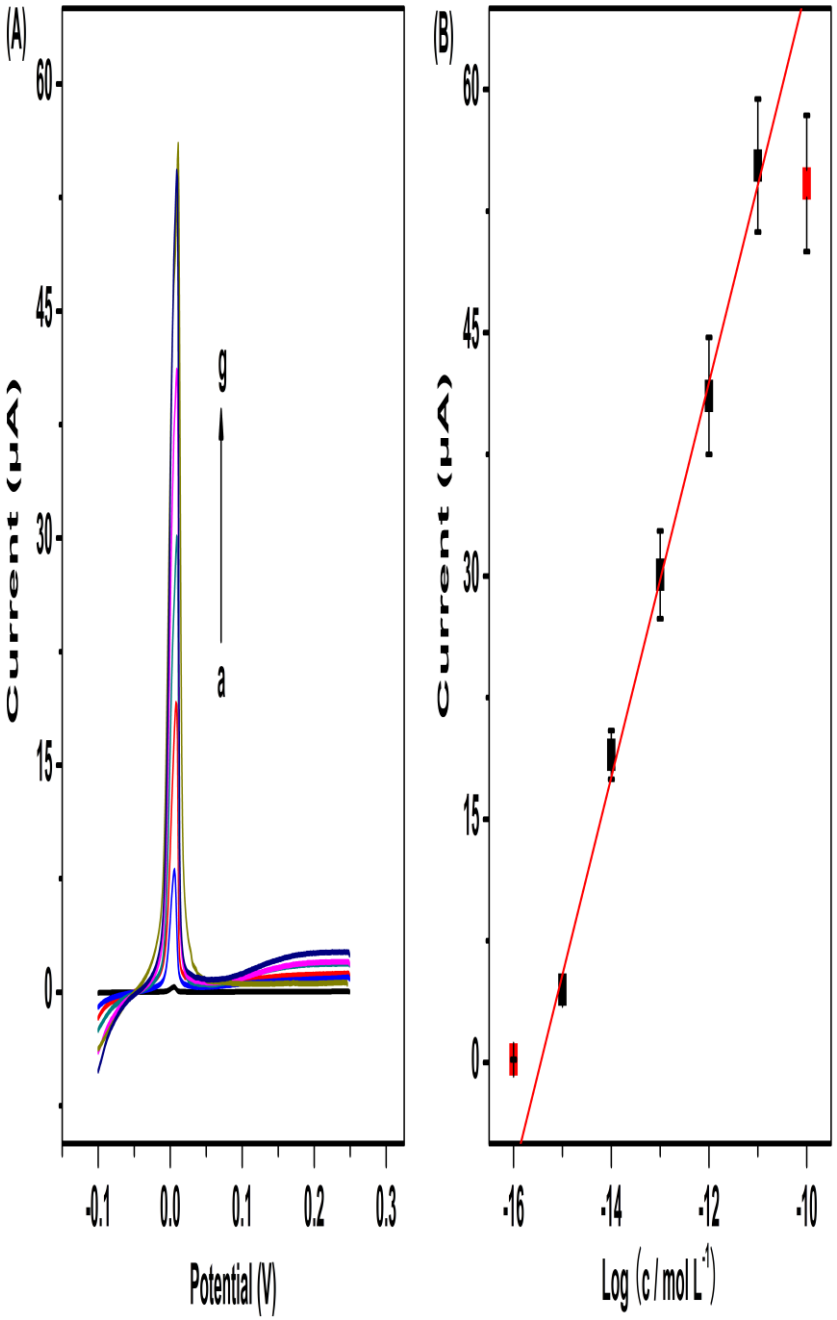
(A)
Current (μA)
60
45
30
15
0
g
a
-0.1
0.0
0.1
0.2
0.3
Potential (V)
(B)
Current (μA)
60
45
30
15
0
-16
-14
-12
-10
Log (c / mol L-1)

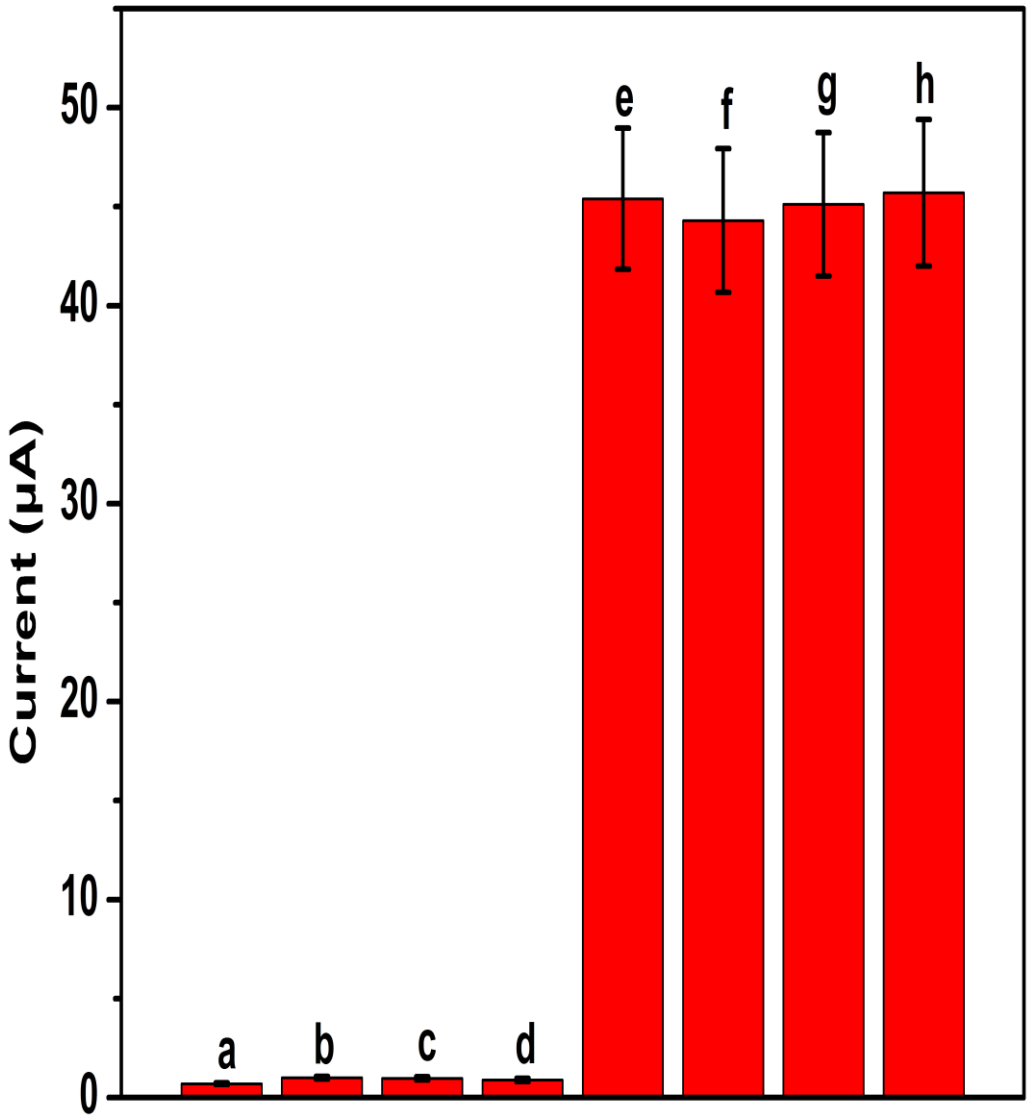

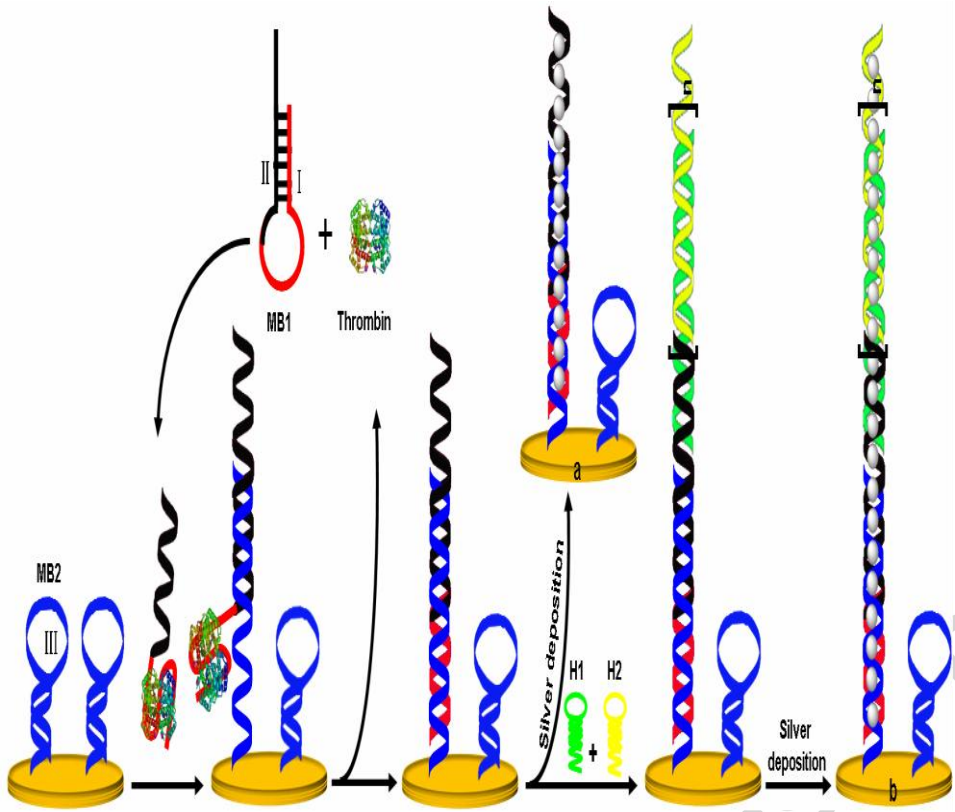

Highlights

► A novel label-free and enzyme-free electrochemical aptasensor for detection of thrombin.

►The signal amplification is based on target catalyzed hairpin assembly, HCR and DNA in situ metallization.

►The biosensor can detect thrombin down to 37 aM level with a dynamic range spanning 5 orders of magnitude.

►The biosensor has high selectivity of thrombin.